The 4th European sCO2 Conference for Energy Systems
23 - 24 March 2021 | ONLINE

2021-sCO2.eu-136

Design and off-design analysis of a highly loaded centrifugal compressor for sCO2 applications operating in near-critical conditions

Alessandro Romei | Paolo Gaetani | Giacomo Persico

POLITECNICO MILANO 1863 ENERGY DEPARTMENT

Laboratory of Fluid Machines

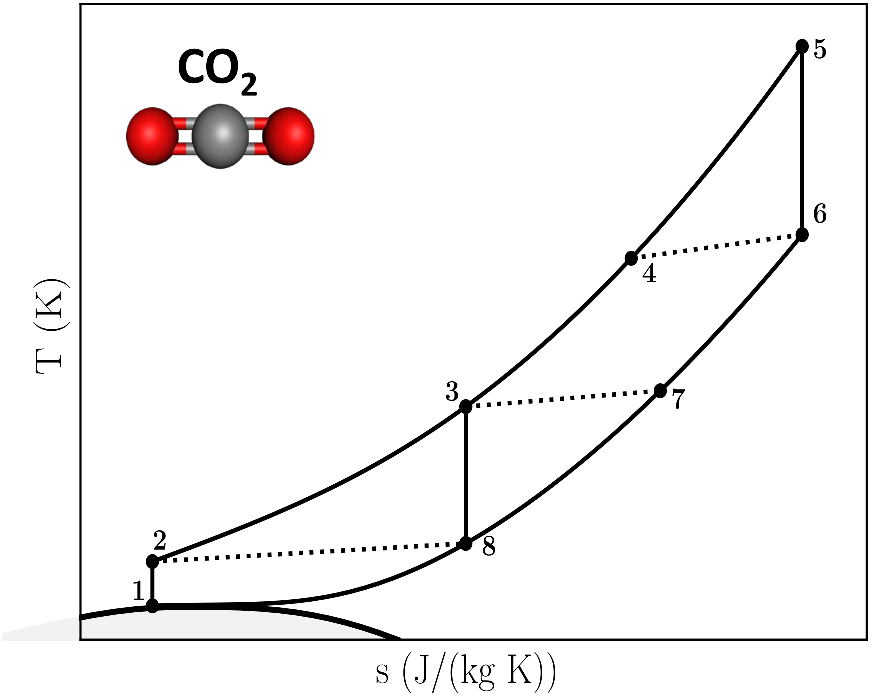

Closed J-B cycles operating with sCO_2

- ✓ Higher conversion efficiency
- ✓ Compact equipment size
- ✓ Faster dynamics

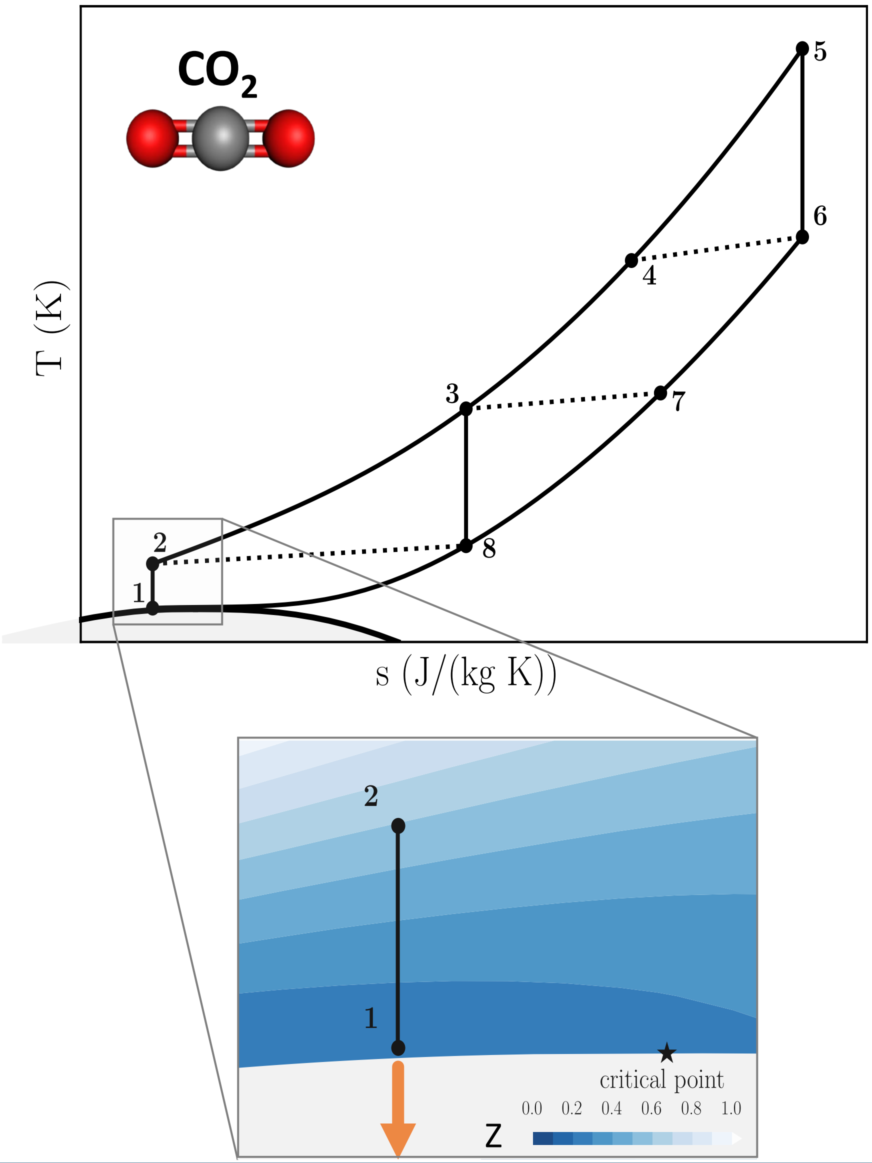

Closed J-B cycles operating with sCO$_2$

- ✓ Higher conversion efficiency
- ✓ Compact equipment size
- ✓ Faster dynamics

But…

…challenges in compressor design!

- ✓ non-ideal fluid thermodynamics
- ✓ two-phase flows
- ✓ size effects

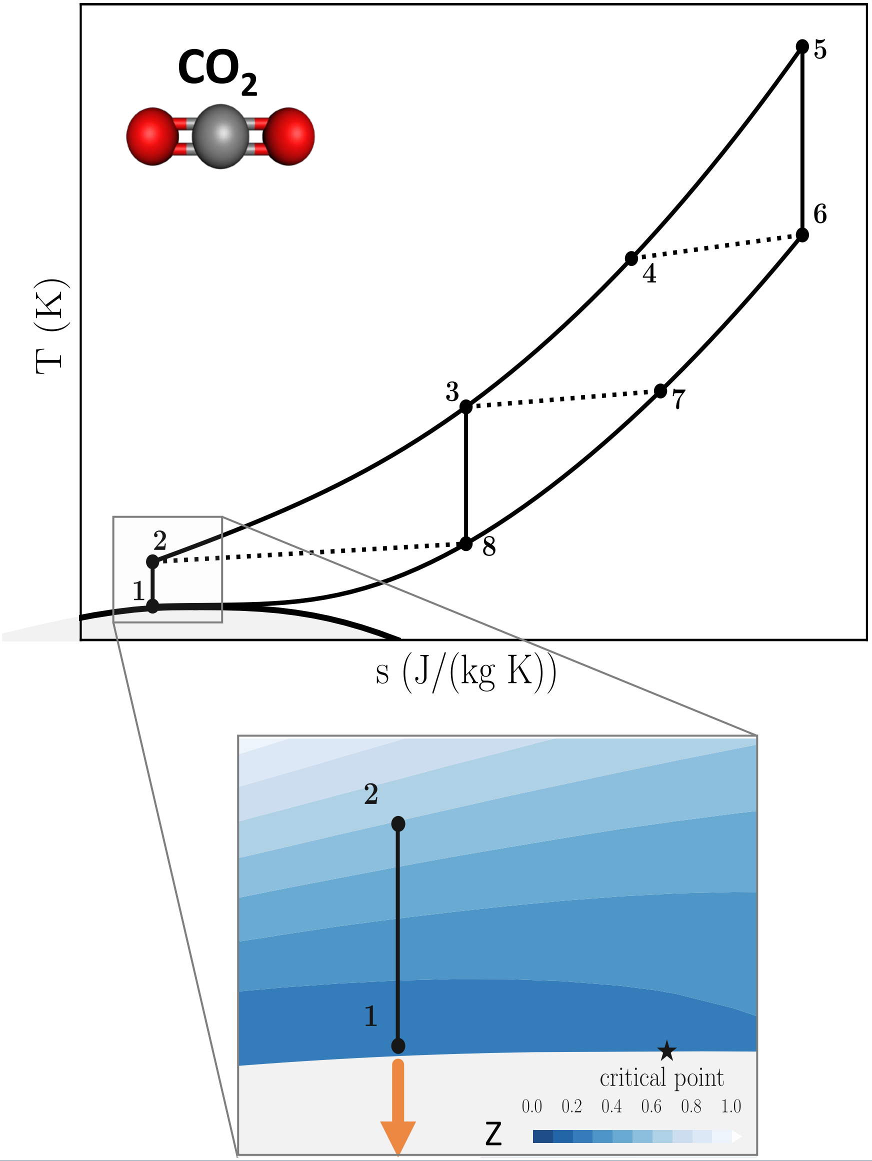

Closed J-B cycles operating with sCO_2

- ✓ Higher conversion efficiency
- ✓ Compact equipment size
- ✓ Faster dynamics

But…

…challenges in compressor design!

- ✓ non-ideal fluid thermodynamics
- ✓ two-phase flows
- ✓ size effects

→ **compressor design & analysis**

Outline

- Selected power system and setting of compressor targets
- Tools for sCO_2 compressor design & analysis: modeling & assessment
  - ✓ Mean-line code for preliminary design and low-fidelity analysis
  - ✓ CFD model for high-fidelity non-ideal two-phase flow simulations
- Compressor design workflow
  - ✓ Constraints and sizing
  - ✓ Aerodynamic blade design
- Compressor aerodynamics and performance
  - ✓ Influence of flow rate and angular speed: compressor maps
  - ✓ Character and implications of phase change
- Conclusions

Application and compressor targets

Recompressed cycle configuration

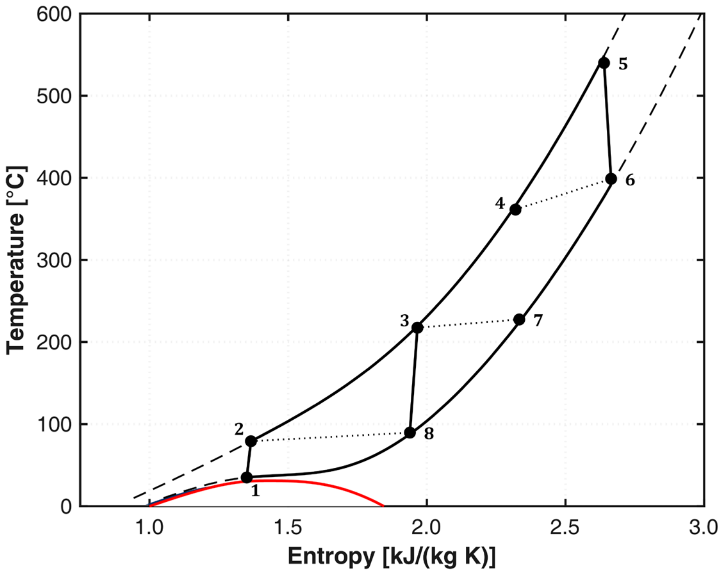

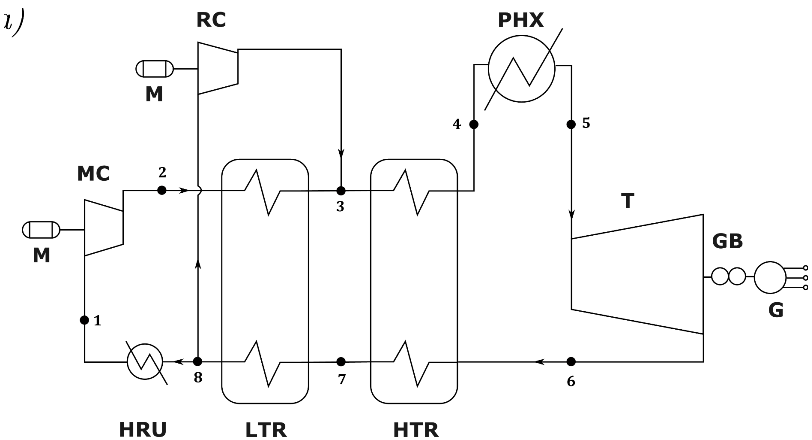

Romei et al., 'The Role of Turbomachinery Performance in the Optimization of sCO_2 Power Systems', JTM 2020

Application and compressor targets

Recompressed cycle configuration

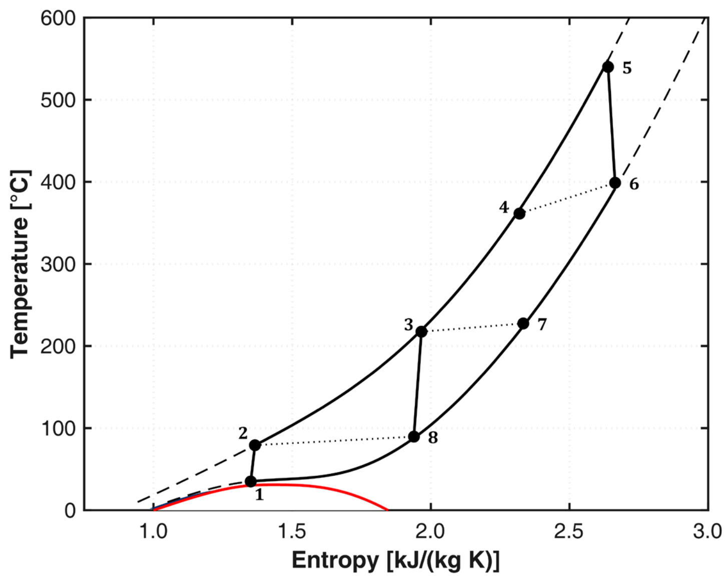

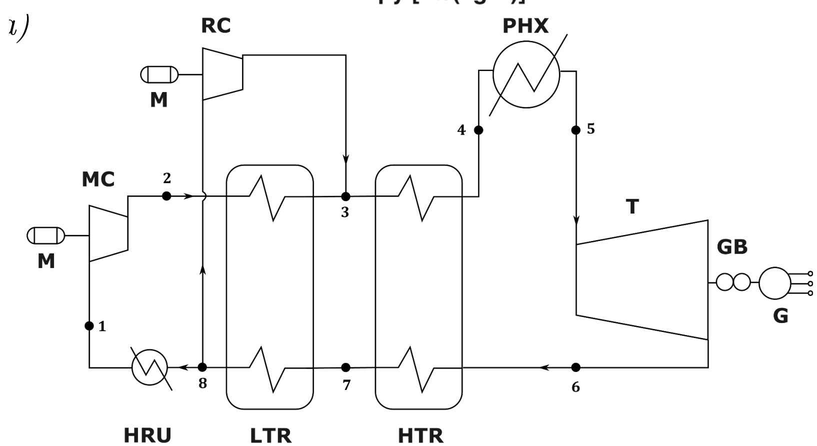

Cycle assumptions

- ✓ T_{hs} = 550°C
- ✓ T_1 = 32°C
- ✓ W = 50 MW (nuclear, CSP)
- ✓ $\Delta T_{PP} = 10°C$
- ✓ $\Delta P/P_{in} = 2\%$
- ✓ $\eta_G = \eta_M = \eta_{GB} = 97\%$

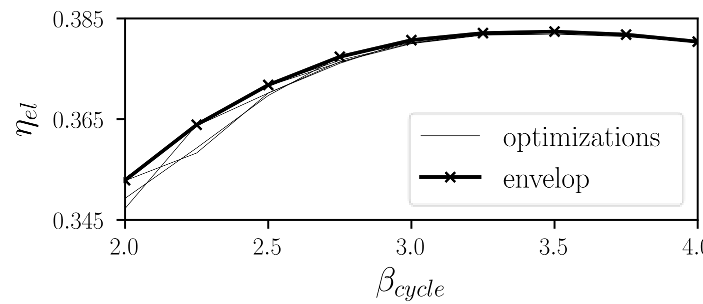

Romei et al., 'The Role of Turbomachinery Performance in the Optimization of sCO_2 Power Systems', JTM 2020

Application and compressor targets

Recompressed cycle configuration

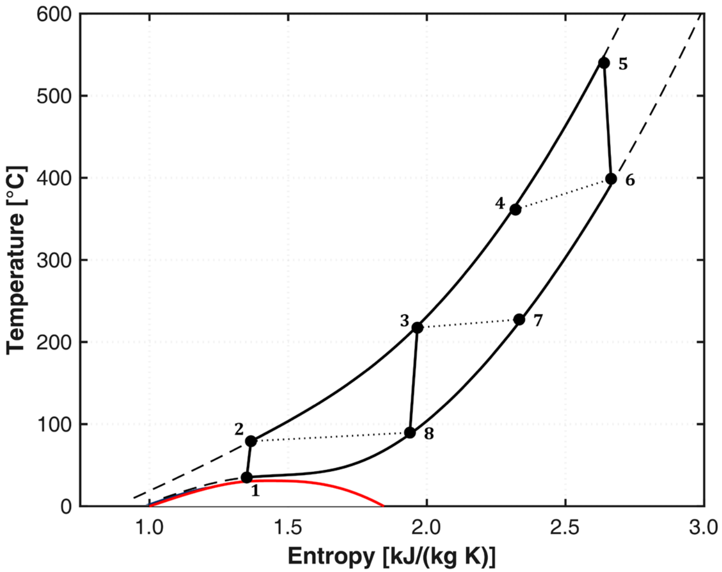

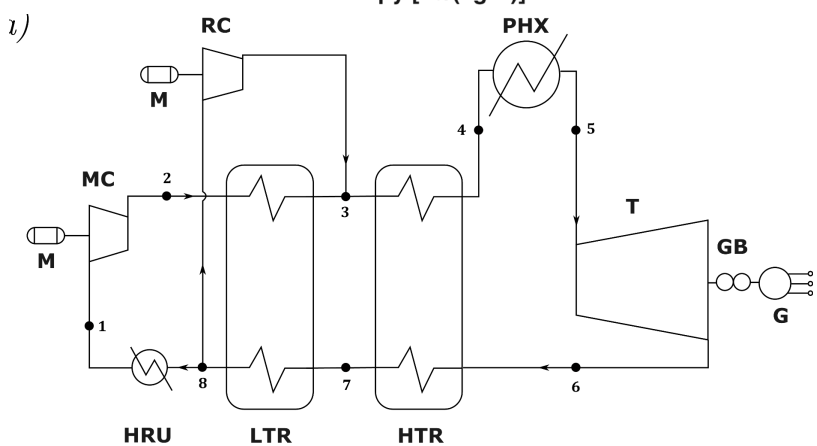

Cycle assumptions

- ✓ T_{hs} = 550°C
- ✓ T_1 = 32°C
- ✓ W = 50 MW (nuclear, CSP)
- ✓ ΔT_{PP} = 10°C
- ✓ $\Delta P/P_{in}$ =2%
- ✓ $\eta_G = \eta_M = \eta_{GB}$ = 97%

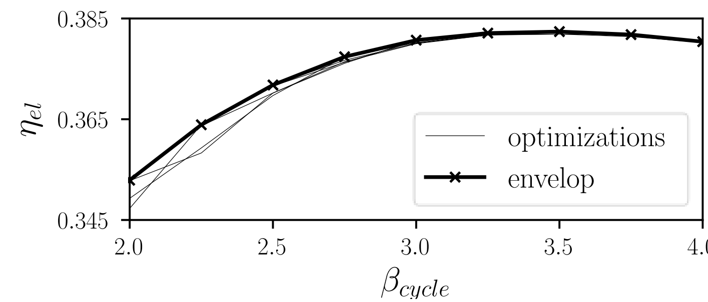

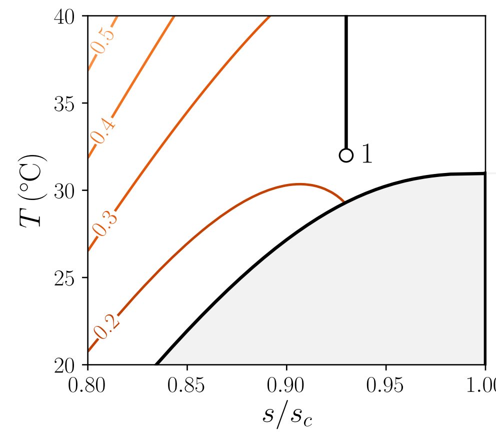

Design conditions	
P_{T1}	78.7 bar
T_{T1}	32 °C
s/s_c	0.93
β	3.25
$\dot{m}$	413.4 kg/s

Romei et al., 'The Role of Turbomachinery Performance in the Optimization of sCO_2 Power Systems', JTM 2020

Outline

- Selected power system and setting of compressor targets
- Tools for sCO_2 compressor design & analysis: modeling & assessment
  - ✓ Mean-line code for preliminary design and low-fidelity analysis
  - ✓ CFD model for high-fidelity non-ideal two-phase flow simulations
- Compressor design workflow
  - ✓ Constraints and sizing
  - ✓ Aerodynamic blade design
- Compressor aerodynamics and performance
  - ✓ Influence of flow rate and angular speed: compressor maps
  - ✓ Character and implications of phase change
- Conclusions

Mean-line code

Impeller and vaneless diffuser

- ✓ Impeller Skin-friction (accounting for roughness and curvature) (Jansen, Aungier, Musgrave)
- ✓ Blade loading and diffusion (Rodgers)
- ✓ Splitter correction (Aungier)
- ✓ Slip factor (Wiesner)
- ✓ Tip Clearance flows (Jansen)
- ✓ Mixing at rotor outlet (Johnston and Dean)
- ✓ Recirculation at rotor outlet (Coppage)
- ✓ Vaneless loss correlation (Stanitz)
- ✓ Incidence (Galvas)

Impeller and vaneless diffuser

- ✓ Impeller Skin-friction (accounting for roughness and curvature) (Jansen, Aungier, Musgrave)
- ✓ Blade loading and diffusion (Rodgers)
- ✓ Splitter correction (Aungier)
- ✓ Slip factor (Wiesner)
- ✓ Tip Clearance flows (Jansen)
- ✓ Mixing at rotor outlet (Johnston and Dean)
- ✓ Recirculation at rotor outlet (Coppage)
- ✓ Vaneless loss correlation (Stanitz)
- ✓ Incidence (Galvas)

Vaned diffuser

- ✓ Diffuser data-book
- ✓ Incidence (Whitfield-Baines)

Mean-line code

Impeller and vaneless diffuser

- ✓ Impeller Skin-friction (accounting for roughness and curvature) (Jansen, Aungier, Musgrave)
- ✓ Blade loading and diffusion (Rodgers)
- ✓ Splitter correction (Aungier)
- ✓ Slip factor (Wiesner)
- ✓ Tip Clearance flows (Jansen)
- ✓ Mixing at rotor outlet (Johnston and Dean)
- ✓ Recirculation at rotor outlet (Coppage)
- ✓ Vaneless loss correlation (Stanitz)
- ✓ Incidence (Galvas)

Vaned diffuser

- ✓ Diffuser data-book
- ✓ Incidence (Whitfield-Baines)

Volute

- ✓ Radial velocity dissipation
- ✓ skin friction

External losses

- ✓ Leakage (Aungier)
- ✓ Disc friction (Aungier), not applied in the present work

Computational framework

CFD solver: Finite Volume ANSYS-CFX with

- ✓ H-R TVD scheme for convective fluxes
- ✓ centred scheme for diffusive terms

Turbulence model: k-ω SST

- ✓ roughness-specific wall functions
- ✓ y^+ defined by sand-grain roughness = 6.2 μm

Mesh: multi-block strcutured with hexahedral cells

Validated against experiments for ideal gas

(Persico et al., 2012, ASME J. Turbomach.)

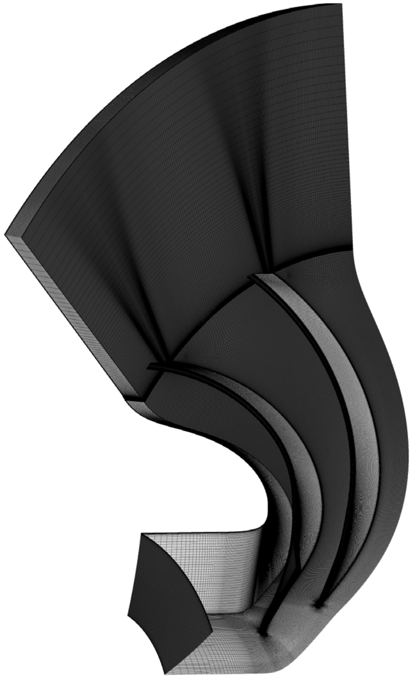

Persico et al., 'Implications of Phase Change on the Aerodynamics of Centrifugal Compressors for sCO2 Applications', JGTP21

CFD model

Computational framework

CFD solver: Finite Volume ANSYS-CFX with
- ✓ H-R TVD scheme for convective fluxes
- ✓ centred scheme for diffusive terms

Turbulence model: k-ω SST
- ✓ roughness-specific wall functions
- ✓ y^+ defined by sand-grain roughness = 6.2 μm

Mesh: multi-block strcutured with hexahedral cells

Validated against experiments for ideal gas
(Persico et al., 2012, ASME J. Turbomach.)

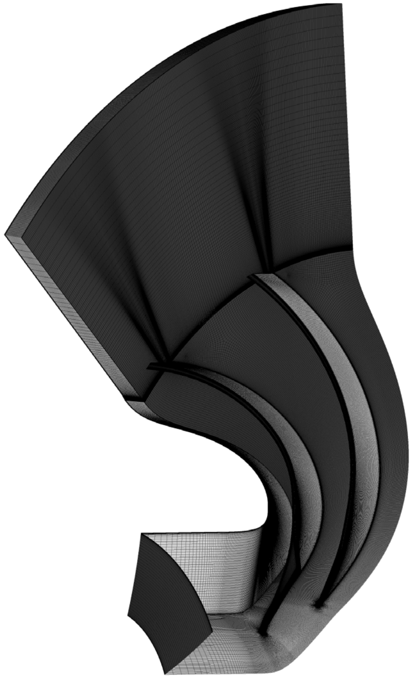

Thermodynamic modeling

LuT based on (P,T) not suitable for two-phase
→ idea: **to assign the pressure-density relation along a pre-defined polytropic with index *n*: *barotropic model***

$$\rho = \rho(P, s) \;\rightarrow\; \rho = \rho(P)\Big|_n$$

Persico et al., 'Implications of Phase Change on the Aerodynamics of Centrifugal Compressors for sCO2 Applications', JGTP21

CFD model

Computational framework

CFD solver: Finite Volume ANSYS-CFX with
- ✓ H-R TVD scheme for convective fluxes
- ✓ centred scheme for diffusive terms

Turbulence model: k-ω SST
- ✓ roughness-specific wall functions
- ✓ y^+ defined by sand-grain roughness = 6.2 μm

Mesh: multi-block strcutured with hexahedral cells

Validated against experiments for ideal gas
(Persico et al., 2012, ASME J. Turbomach.)

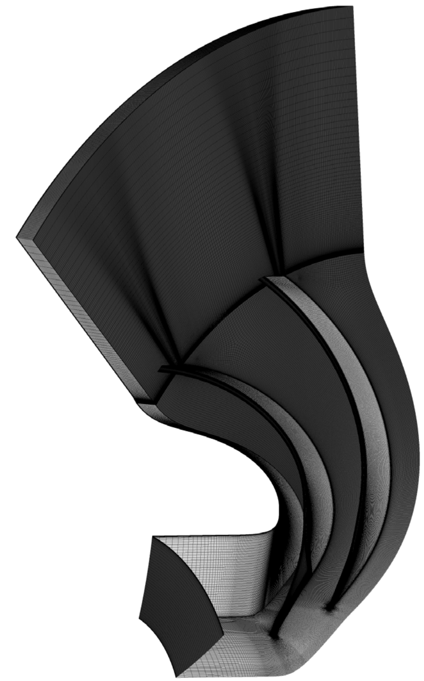

Thermodynamic modeling

LuT based on (P,T) not suitable for two-phase

→ idea: **to assign the pressure-density relation along a pre-defined polytropic with index *n*: *barotropic model***

$$\rho = \rho(P, s) \rightarrow \rho = \rho(P)\Big|_n$$

Two polynomials interpolate the single phase and two-phase regions, linked by a logistic function

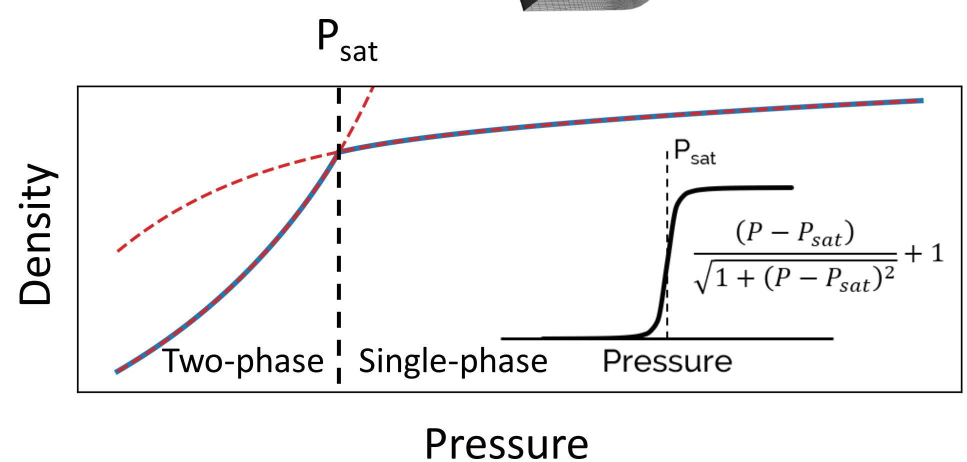

Persico et al., 'Implications of Phase Change on the Aerodynamics of Centrifugal Compressors for sCO2 Applications', JGTP21

CFD Barotropic model assessment

Experimental validation for
CAVITATING FLOWS
in converging-diverging nozzle
$s/s_c = 0.95$; $P_{T,in} = 91$ bar

Nakagawa *et. al.*, "Supersonic two-phase..", *Int. J. Refr.*, 2009

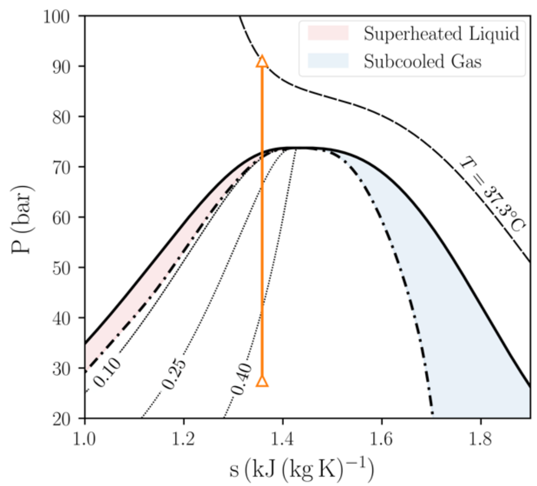

Romei and Persico, 'CFD modeling of compressible two phase flows of CO2 in superctitical conditions', ATE 2021

CFD Barotropic model assessment

Experimental validation for
CAVITATING FLOWS
in converging-diverging nozzle
$s/s_c = 0.95$; $P_{T,in} = 91$ bar

Nakagawa *et. al.*, "Supersonic two-phase..", *Int. J. Refr.*, 2009

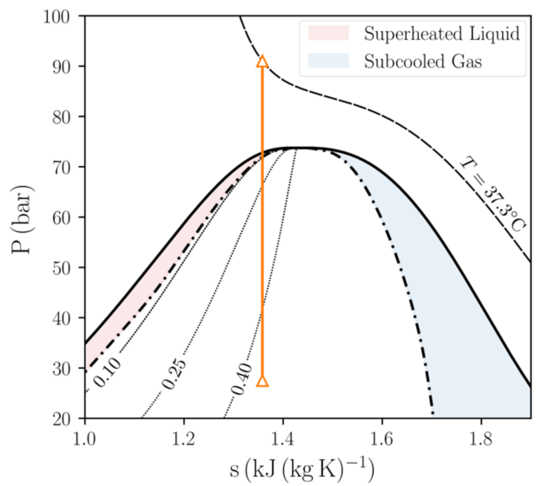

Two CFD simulation models

- ✓ Barotropic model with isentropic P-ρ law
- ✓ Mixture model as a complete HEM (i.e. including thermal effects)

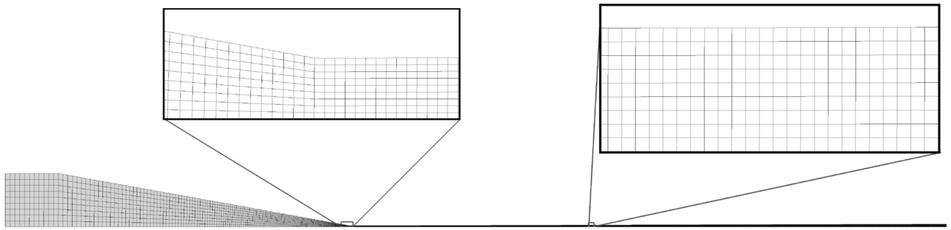

Romei and Persico, 'CFD modeling of compressible two phase flows of CO2 in superctitical conditions', ATE 2021

CFD Barotropic model assessment

Experimental validation for **CAVITATING FLOWS** in converging-diverging nozzle

$s/s_c = 0.95; P_{T,in} = 91$ bar

Nakagawa *et. al.*, "Supersonic two-phase..", *Int. J. Refr.*, 2009

Two CFD simulation models

- ✓ Barotropic model with isentropic P-ρ law
- ✓ Mixture model as a complete HEM (i.e. including thermal effects)

Excellent agreement between models and experiment

- ✓ In terms of pressure and temperature
- ✓ in terms of liquid mass fraction

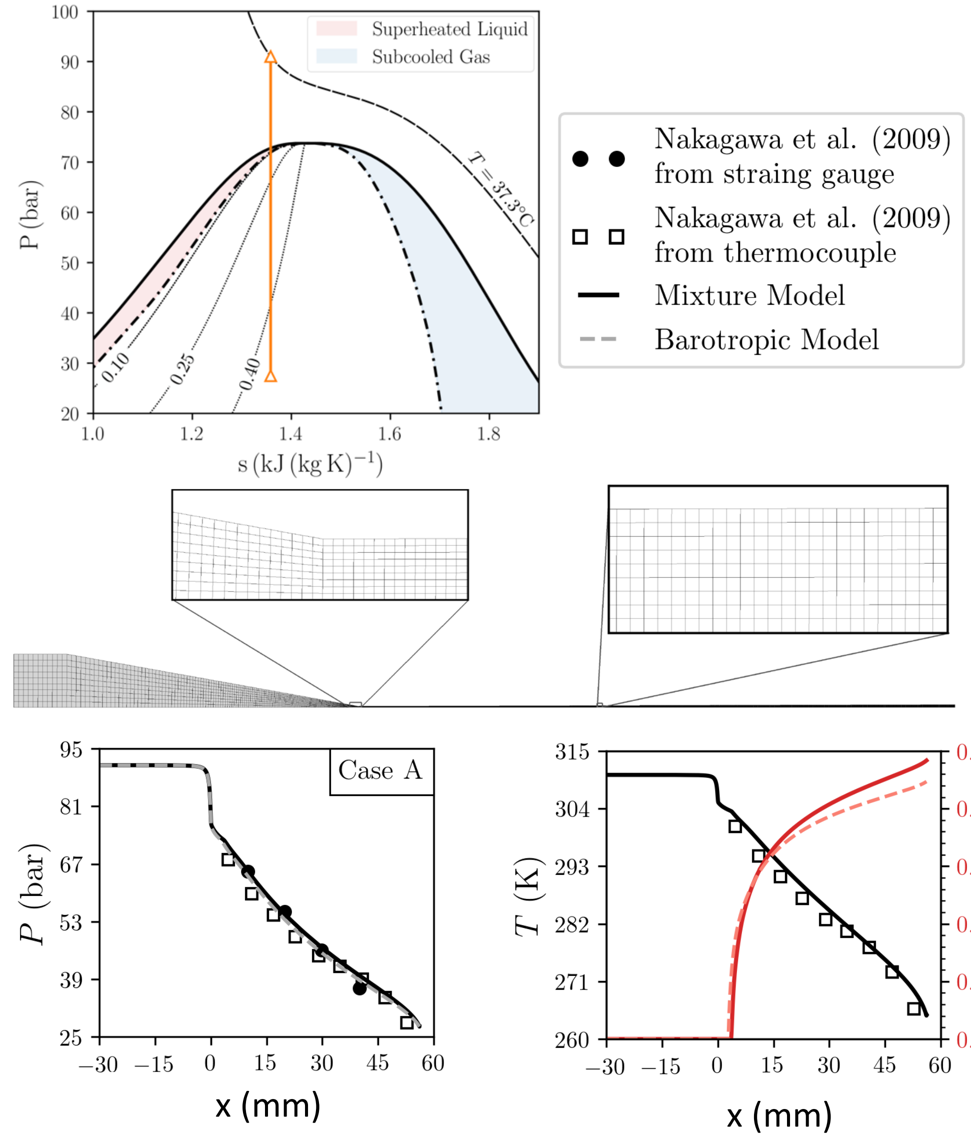

Romei and Persico, 'CFD modeling of compressible two phase flows of CO2 in superctitical conditions', ATE 2021

CFD Barotropic model assessment

Experimental validation for **CAVITATING FLOWS** in converging-diverging nozzle

$s/s_c = 0.95$; $P_{T,in} = 91$ bar

Nakagawa *et. al.*, "Supersonic two-phase..", *Int. J. Refr.*, 2009

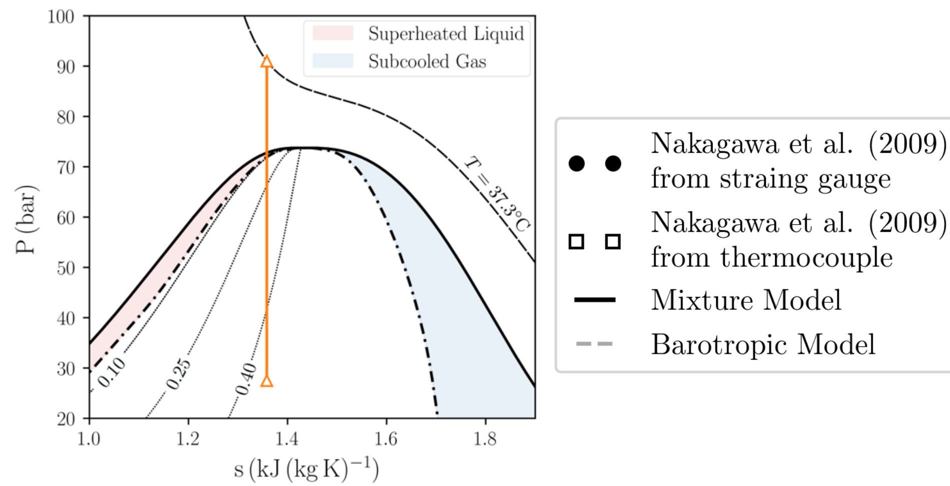

Two CFD simulation models

- ✓ Barotropic model with isentropic P-ρ law
- ✓ Mixture model as a complete HEM (i.e. including thermal effects)

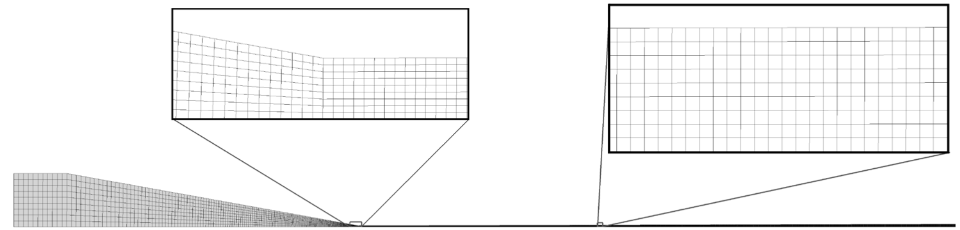

Excellent agreement between models and experiment

- ✓ In terms of pressure and temperature
- ✓ in terms of liquid mass fraction

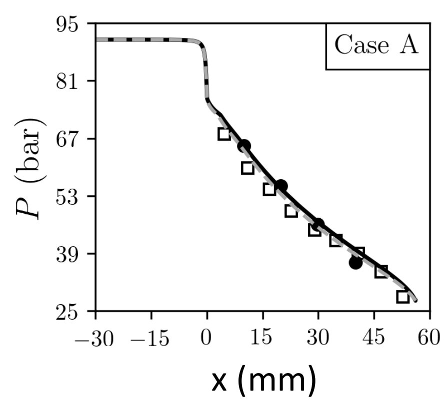

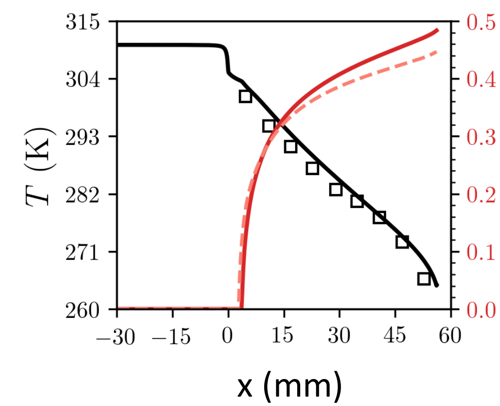

Conclusions on CFD model

- ✓ Entropy production not fixed by P-ρ law
- ✓ Real-gas volumetric behaviour predicted
- ✓ Robust and cheaper than mixture model

Romei and Persico, 'CFD modeling of compressible two phase flows of CO2 in superctitical conditions', ATE 2021

Outline

- Selected power system and setting of compressor targets
- Tools for sCO2 compressor design & analysis: modeling & assessment
  - ✓ Mean-line code for preliminary design and low-fidelity analysis
  - ✓ CFD model for high-fidelity non-ideal two-phase flow simulations
- Compressor design workflow
  - ✓ Constraints and sizing
  - ✓ Aerodynamic blade design
- Compressor aerodynamics and performance
  - ✓ Influence of flow rate and angular speed: compressor maps
  - ✓ Character and implications of phase change
- Conclusions

sCO2 compressor sizing

Design space / constraints

- ✓ 12 < Nb < 18 (w/wo splitters)
- ✓ 8000 [rpm] < n < 13000 [rpm]
- ✓ $-80° < \beta_{1g} < -10°$
- ✓ $-55° < \beta_{2g} < -35°$
- ✓ $60° < \alpha_2 < 75°$
- ✓ Unshrouded imp. (tc = 0.5mm)
- ✓ $D_{1h} = 1.08\ D_{shaft}$

Objectives

- ✓ Minimize M_{w1t}
- ✓ Maximize efficiency
- ✓ Avoid blockage-induced phase change

sCO2 compressor sizing

Design space / constraints

- ✓ 12 < Nb < 18 (w/wo splitters)
- ✓ 8000 [rpm] < n < 13000 [rpm]
- ✓ -80° < β_{1g} < -10°
- ✓ −55° < β_{2g} < −35°
- ✓ 60° < α_2 < 75°
- ✓ Unshrouded imp. (tc = 0.5mm)
- ✓ $D_{1h} = 1.08\ D_{shaft}$

Objectives

- ✓ Minimize M_{w1t}
- ✓ Maximize efficiency
- ✓ Avoid blockage-induced phase change

Preliminary sizing

- ✓ D_{1h} = 90 mm
- ✓ Nb = 8 + 8 splitter (s_{NORM} = 0.175)
- ✓ n_{des} = 10000 [rpm]
- ✓ β_{1g} = -43.1 (h), -53.7° (m), -60.5° (t)
- ✓ β_{2g} = −45°
- ✓ α_2 = 73.4°
- ✓ η_{TT} = 84.7°

Design condition

ϕ_{des} = 0.21

$M_{u2,des}$ = 0.86

$Re_{des} = 10^9$

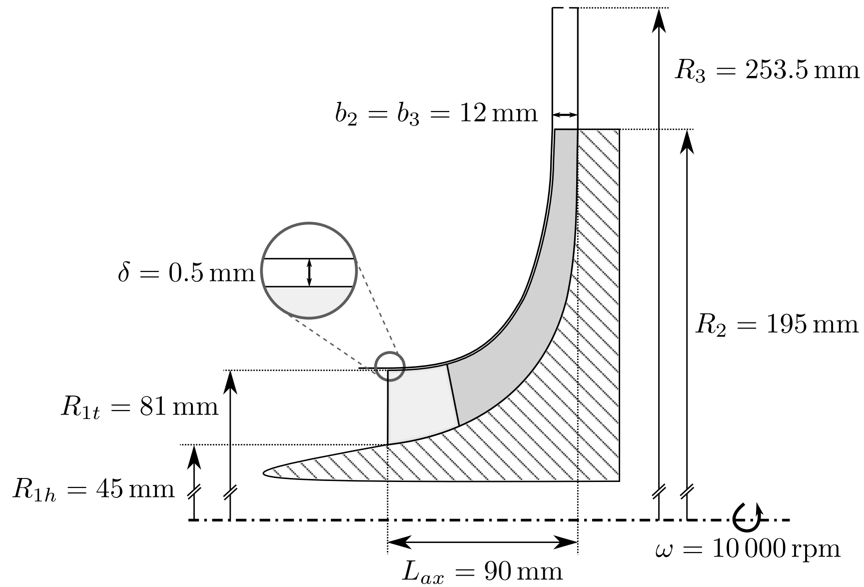

Blade camberline and thickness

- ✓ Crucial for controlling diffusion
- ✓ Crucial for minimizing front suction

Role of wrap angle φ

- ✓ Effective way to distribute cambering
- ✓ Impact on throat section at the inlet

Blade camberline and thickness

- ✓ Crucial for controlling diffusion
- ✓ Crucial for minimizing front suction

Role of wrap angle φ

- ✓ Effective way to distribute cambering
- ✓ Impact on throat section at the inlet

Low wrap angle (a)

- ✓ Higher suction → higher risk of local phase change on blade suction side
- ✓ Large throat → low risk of blockage-induced phase change

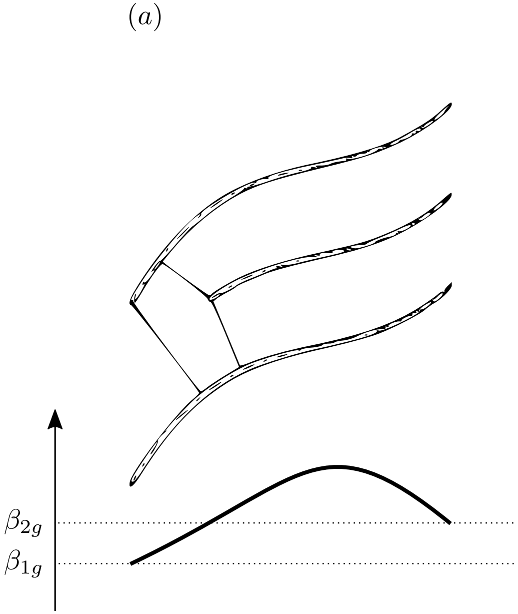

sCO2 compressor aerodynamic design

Blade camberline and thickness

- ✓ Crucial for controlling diffusion
- ✓ Crucial for minimizing front suction

Role of wrap angle φ

- ✓ Effective way to distribute cambering
- ✓ Impact on throat section at the inlet

Low wrap angle (a)

- ✓ Higher suction → higher risk of local phase change on blade suction side
- ✓ Large throat → low risk of blockage-induced phase change

High wrap angle (b)

- ✓ Lower suction → lower risk of local phase change on blade suction side
- ✓ Small throat → high risk of blockage-induced phase change

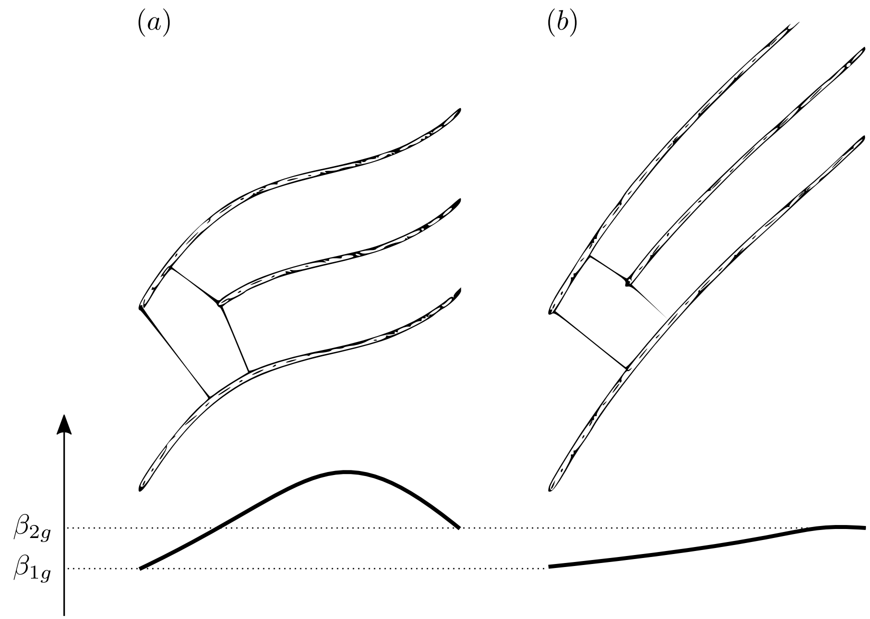

Blade camberline and thickness

- ✓ Crucial for controlling diffusion
- ✓ Crucial for minimizing front suction

Role of wrap angle φ

- ✓ Effective way to distribute cambering
- ✓ Impact on throat section at the inlet

Low wrap angle (a)

- ✓ Higher suction → higher risk of local phase change on blade suction side
- ✓ Large throat → low risk of blockage-induced phase change

High wrap angle (b)

- ✓ Lower suction → lower risk of local phase change on blade suction side
- ✓ Small throat → high risk of blockage-induced phase change

Selected wrap angle φ = 85°

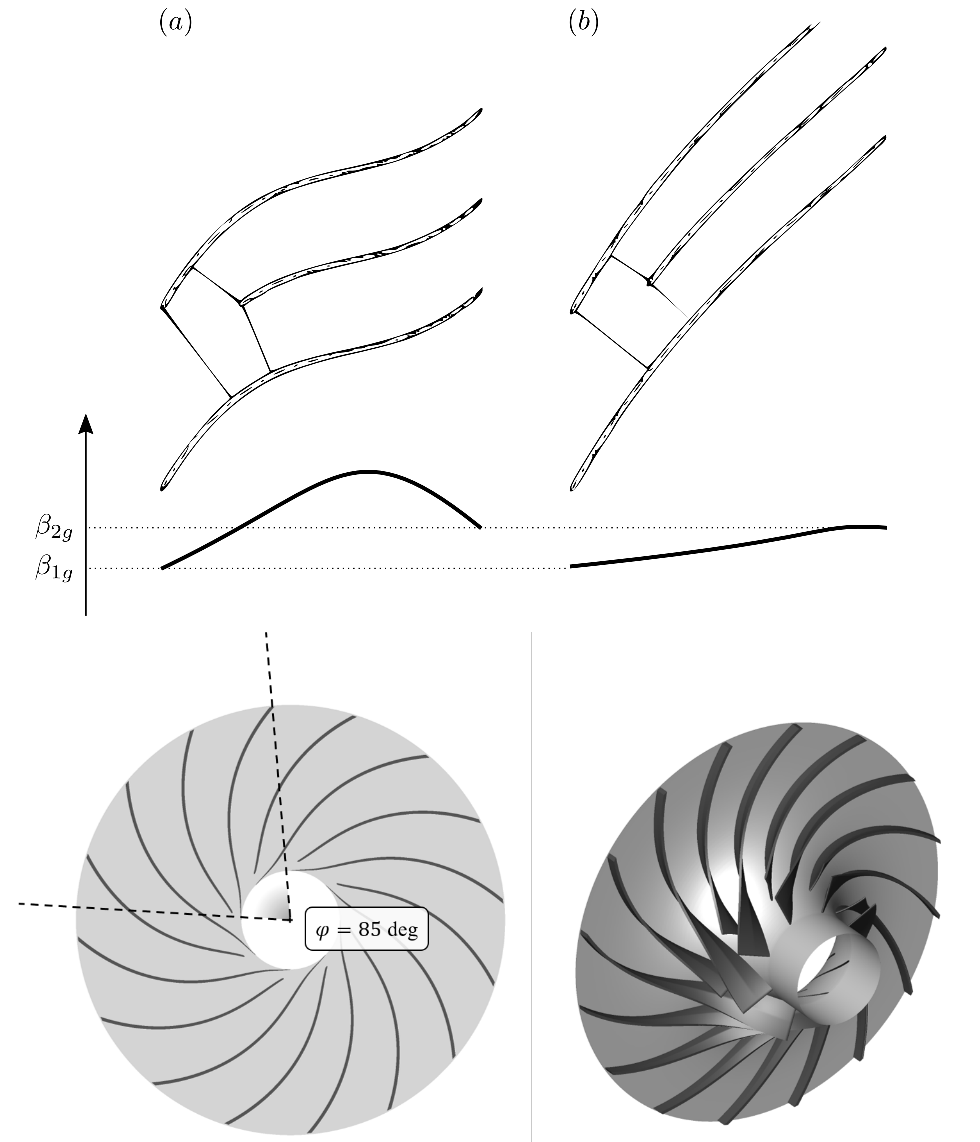

CFD Assessment in design condition

CFD mesh assessment

	Coarse	Medium	Fine
Hub BL	9	13	18
Shroud BL	9	13	18
Tip Clearance	9	18	28
Overall span	40	70	100
Bl2Bl Impeller	25,000	75,000	150,000
Overall	1.9×10^6	8.8×10^6	2.4×10^7

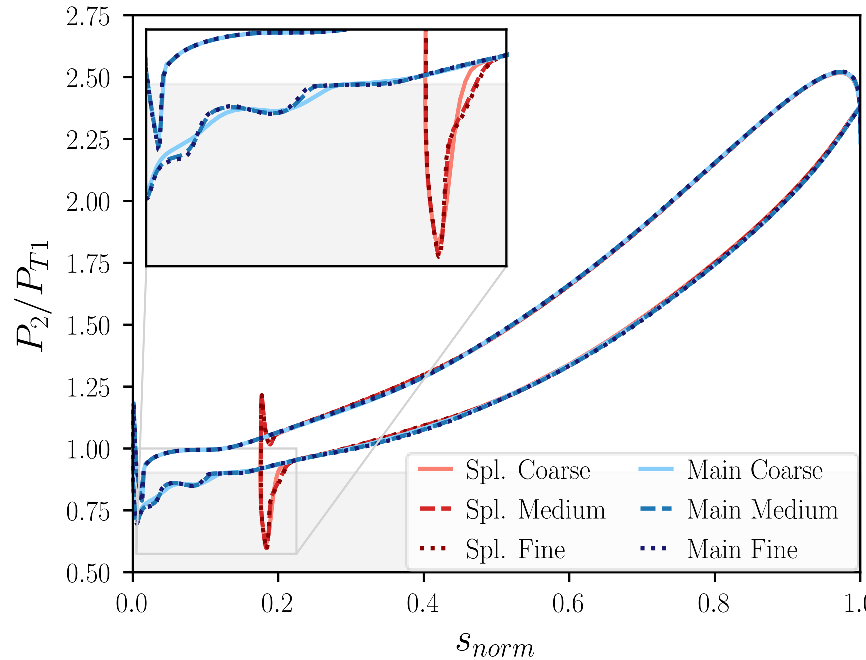

✓ $\Delta\eta_{TT} < 0.1\%$ among meshes, differences on pressure distribution
→ **medium mesh** ultimately selected

CFD Assessment in design condition

CFD mesh assessment

	Coarse	Medium	Fine
Hub BL	9	13	18
Shroud BL	9	13	18
Tip Clearance	9	18	28
Overall span	40	70	100
Bl2Bl Impeller	25,000	75,000	150,000
Overall	1.9×10^6	8.8×10^6	2.4×10^7

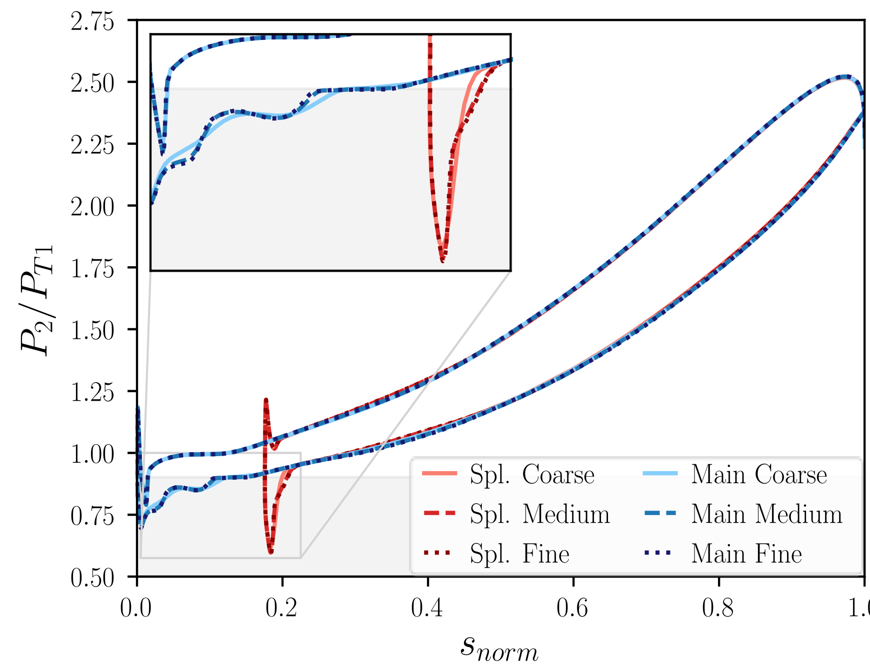

- ✓ $\Delta\eta_{TT}$ < 0.1% among meshes, differences on pressure distribution → **medium mesh** ultimately selected

- ✓ $\Delta\eta_{TT}$ between mean-line and CFD < 2%
- ✓ $\Delta\beta_{TT}$ between mean-line and CFD < 0.2%

Outline

- Selected power system and setting of compressor targets
- Tools for sCO2 compressor design & analysis: modeling & assessment
  - ✓ Mean-line code for preliminary design and low-fidelity analysis
  - ✓ CFD model for high-fidelity non-ideal two-phase flow simulations
- Compressor design workflow
  - ✓ Constraints and sizing
  - ✓ Aerodynamic blade design
- Compressor aerodynamics and performance
  - ✓ Influence of flow rate and angular speed: compressor maps
  - ✓ Character and implications of phase change
- Conclusions

Compressor impeller maps

Three speed-lines considered

- ✓ Nominal speed 100% ω_{des} ($M_{u2,des} = 0.86$)
- ✓ Intermediate speed 80% ω_{des} ($M_{u2} = 0.69$)
- ✓ Low speed 60% ω_{des} ($M_{u2} = 0.52$)

Mean-line prediction

- ✓ Conventional dependence of β_{TT} on ω
- ✓ Weak impact on η_{TT} (no Re, weak M effects)
- ✓ Subsonic flow predicted for any condition
- ✓ Apparent wide rangeability

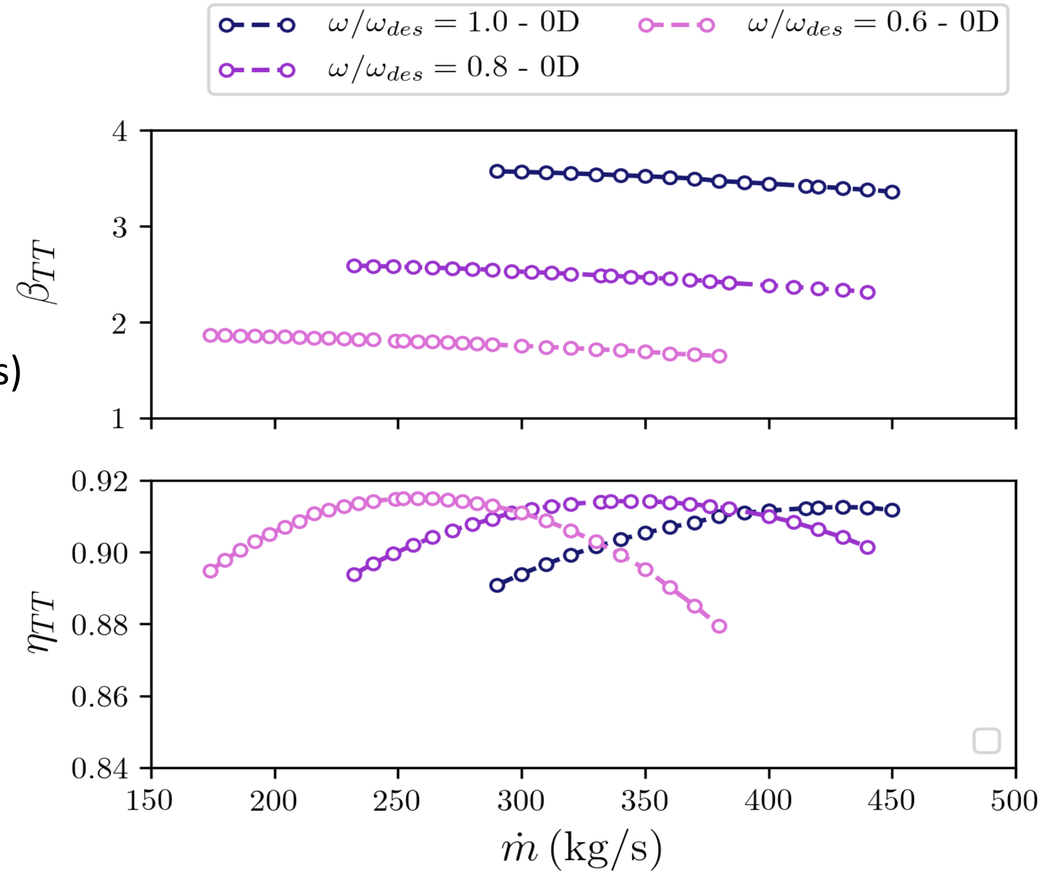

Compressor impeller maps

Three speed-lines considered

- ✓ Nominal speed 100% ω_{des} ($M_{u2,des}$ = 0.86)
- ✓ Intermediate speed 80% ω_{des} (M_{u2} = 0.69)
- ✓ Low speed 60% ω_{des} (M_{u2} = 0.52)

Mean-line prediction

- ✓ Conventional dependence of β_{TT} on ω
- ✓ Weak impact on η_{TT} (no Re, weak M effects)
- ✓ Subsonic flow predicted for any condition
- ✓ Apparent wide rangeability

CFD simulations

- ✓ Very good agreement in terms of β_{TT}
- ✓ Larger deviations in terms of η_{TT}
- ✓ Amplification of loss at low flow rate
- ✓ Abrupt performance drop at high flow rate

→ **Choking occurs!**

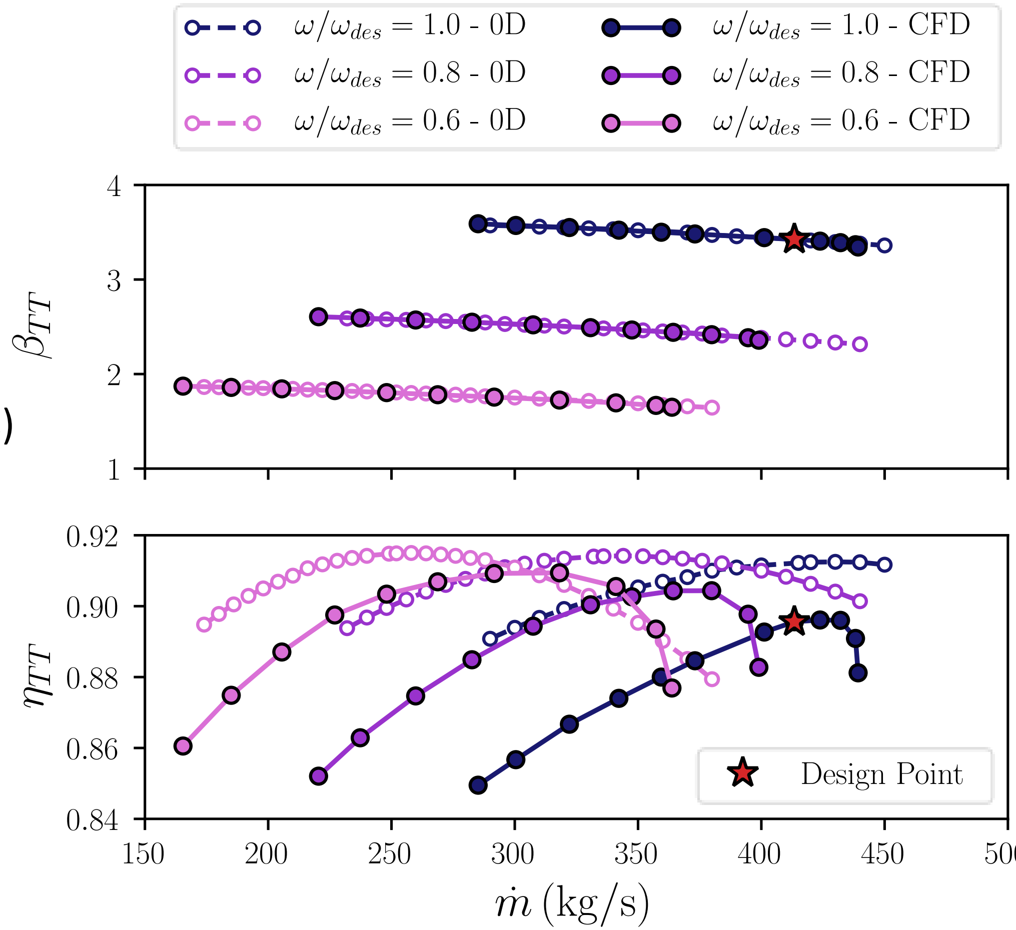

Character of phase change at design conditions

- ✓ Pressure/density field processed to obtain the liquid mass fraction
- ✓ Two-phase flow appear as non-uniform flow areas featuring mixed properties (two-fluid model)
- ✓ Phase change on **front suction side** due to camber and on **splitter LE** due to incidence

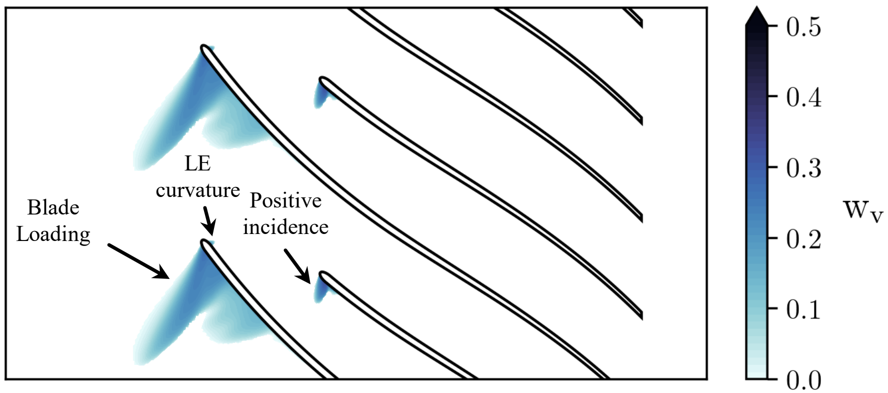

Character of phase change at design conditions

- ✓ Pressure/density field processed to obtain the liquid mass fraction
- ✓ Two-phase flow appear as non-uniform flow areas featuring mixed properties (two-fluid model)
- ✓ Phase change on **front suction side** due to camber and on **splitter LE** due to incidence
- ✓ Supersonic flows are triggered in these areas due to the drop of speed of sound

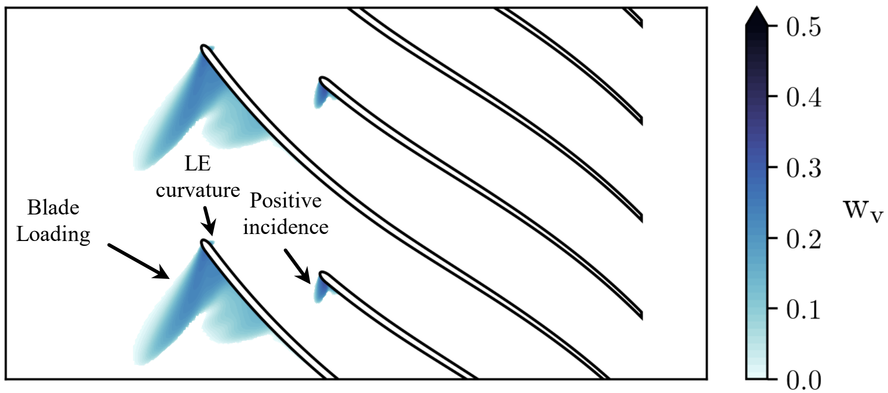

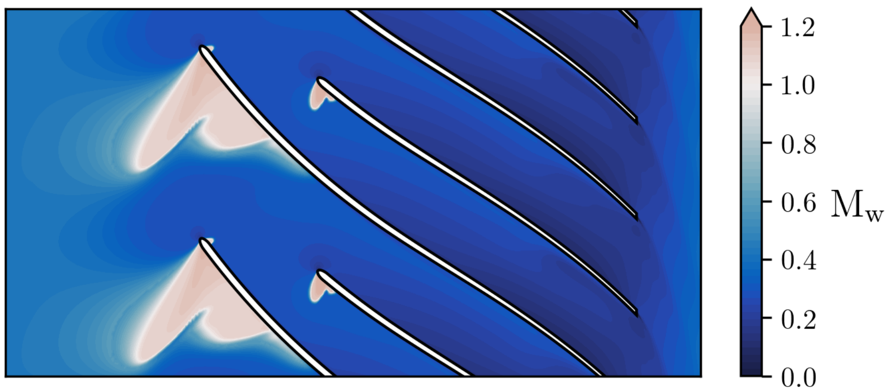

Character of phase change at design conditions

- ✓ Pressure/density field processed to obtain the liquid mass fraction
- ✓ Two-phase flow appear as non-uniform flow areas featuring mixed properties (two-fluid model)
- ✓ Phase change on **front suction side** due to camber and on **splitter LE** due to incidence
- ✓ Supersonic flows are triggered in these areas due to the drop of speed of sound
- ✓ Effects magnified at blade tip (isosurface of saturated pressure)

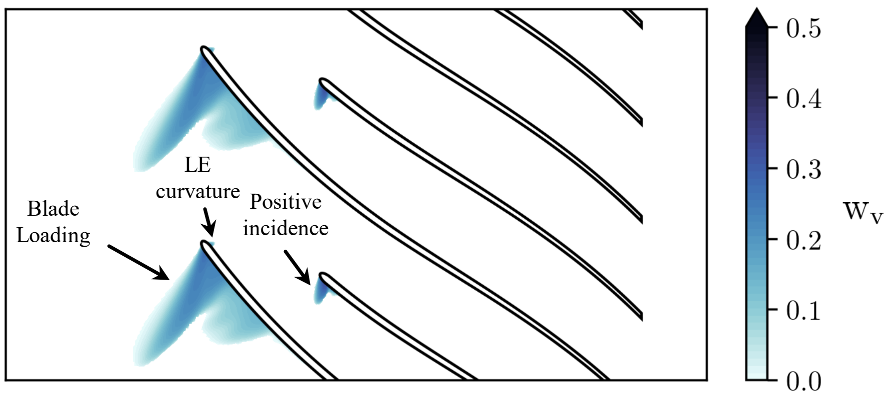

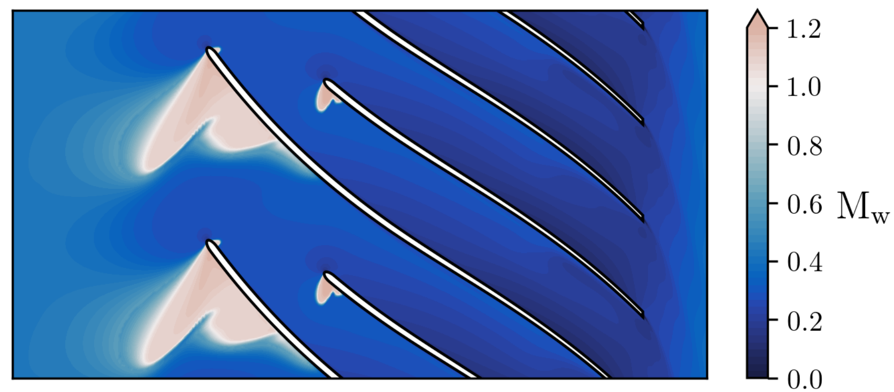

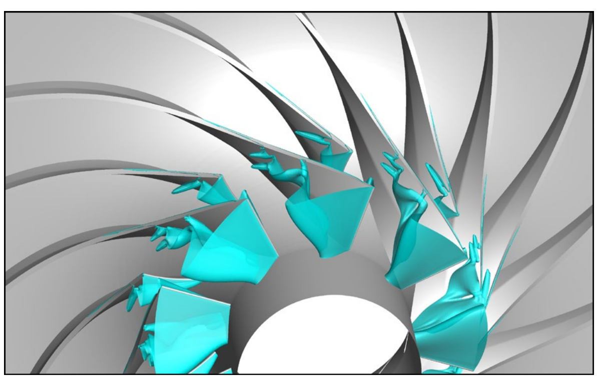

100% ω_{des}

Character of phase change at design conditions

- ✓ Pressure/density field processed to obtain the liquid mass fraction
- ✓ Two-phase flow appear as non-uniform flow areas featuring mixed properties (two-fluid model)
- ✓ Phase change on **front suction side** due to camber and on **splitter LE** due to incidence
- ✓ Supersonic flows are triggered in these areas due to the drop of speed of sound
- ✓ Effects magnified at blade tip (isosurface of saturated pressure)
- ✓ Two-phase flows drastically limited by reducing the angular speed

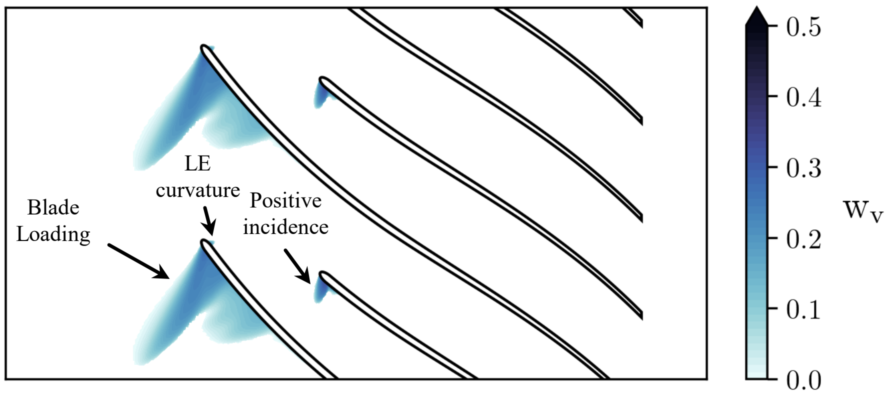

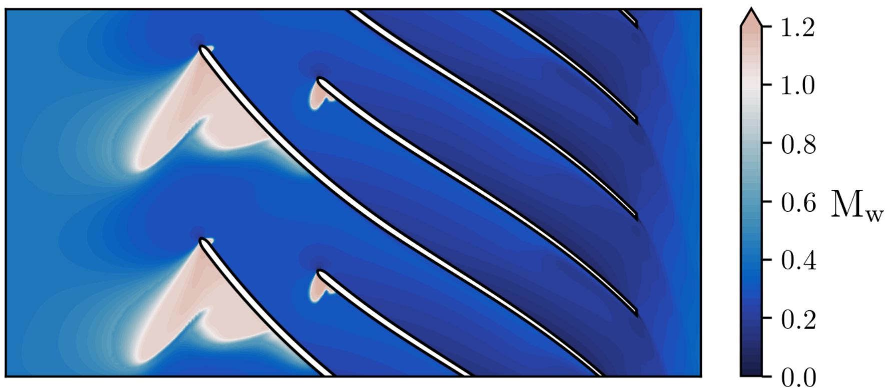

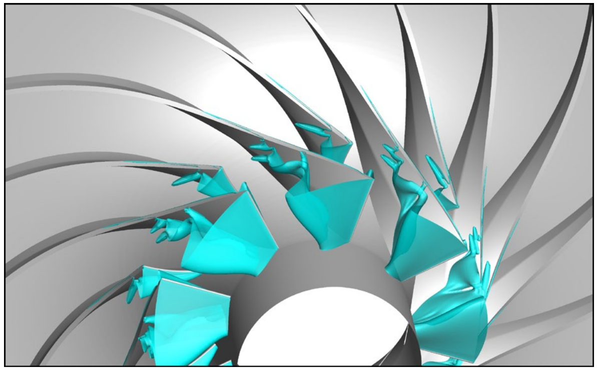

100% ω_{des}

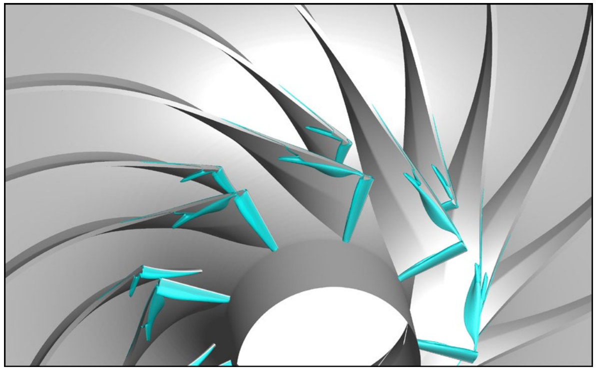

80% ω_{des}

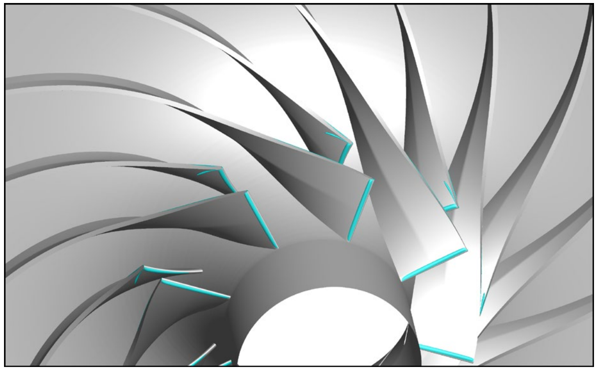

60% ω_{des}

Impact of phase change on rangeability

- ✓ For $\phi/\phi_{des} < 1$ only local two-phase effects, due to incidence, no choking and regular trends
  - ✓ For $\phi/\phi_{des} > 1$ cavitation-induced choking occurs abruptly, triggered by suction

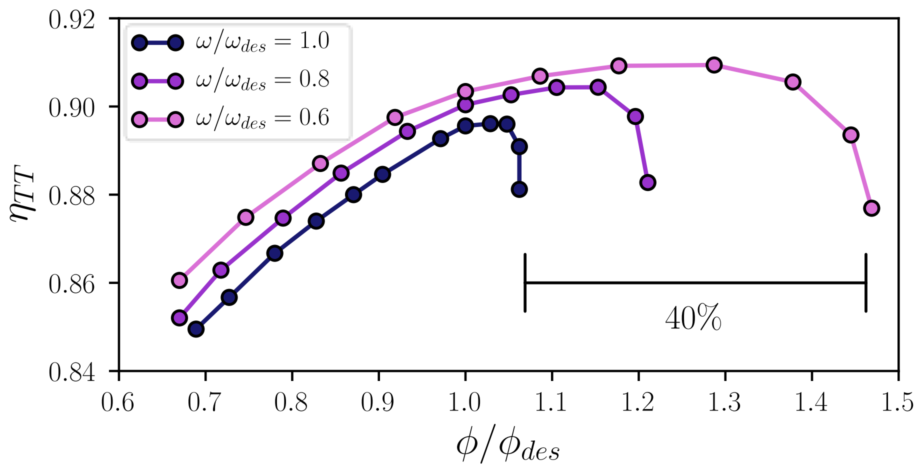

Impact of phase change on rangeability

- ✓ For $\phi/\phi_{des} < 1$ only local two-phase effects, due to incidence, no choking and regular trends
  - ✓ For $\phi/\phi_{des} > 1$ cavitation-induced choking occurs abruptly, triggered by suction
- ✓ At low ω choking occurs at at $\phi/\phi_{des} = 1.45$: negative incidence combines with suction

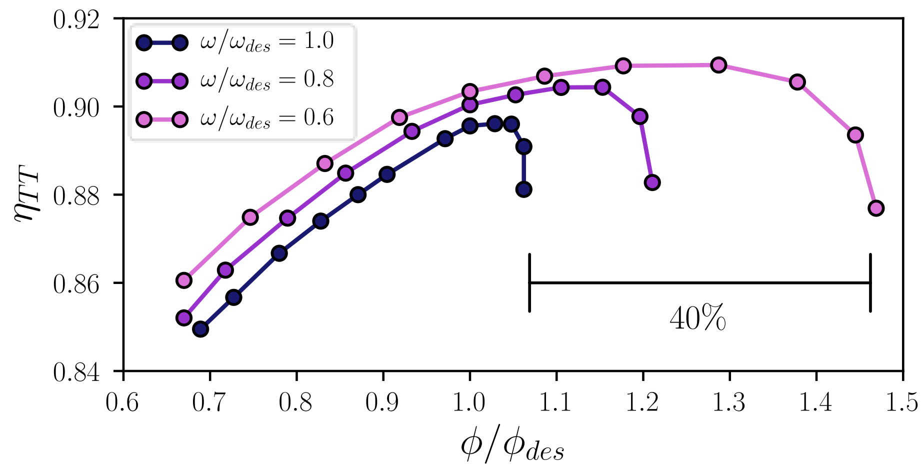

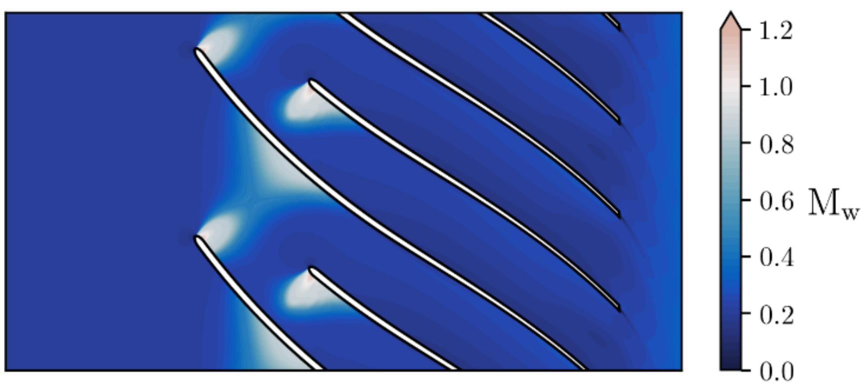

$\phi/\phi_{des} = 1.38$; $\omega/\omega_{des} = 0.6$

Impact of phase change on rangeability

- ✓ For $\phi/\phi_{des} < 1$ only local two-phase effects, due to incidence, no choking and regular trends
- ✓ For $\phi/\phi_{des} > 1$ cavitation-induced choking occurs abruptly, triggered by suction
- ✓ At low ω choking occurs at at $\phi/\phi_{des} = 1.45$: negative incidence combines with suction
- ✓ At ω_{des} choking occurs at $\phi/\phi_{des} = 1.06$: two phase region quickly covers the entire channel

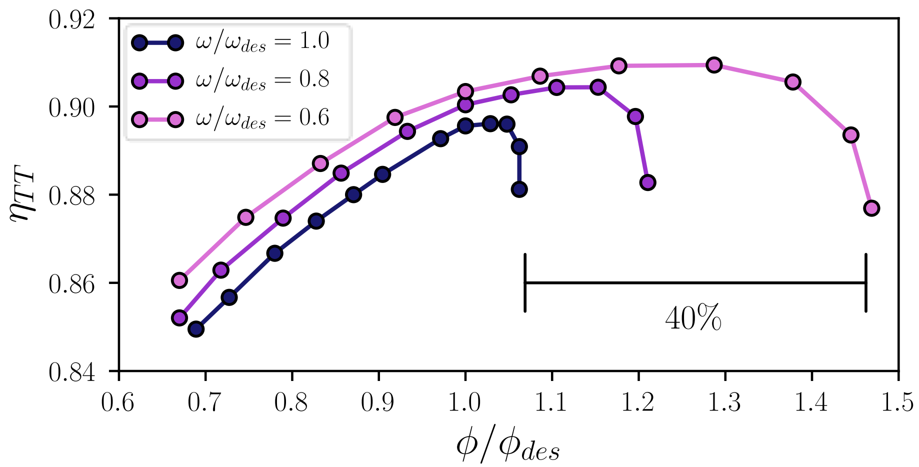

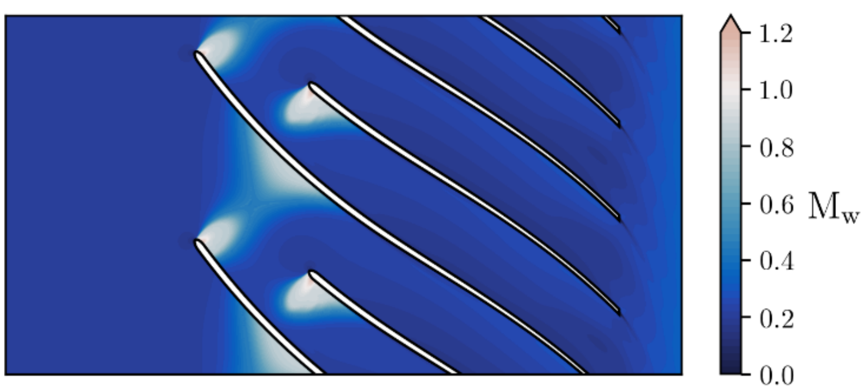

$\phi/\phi_{des} = 1.38$; $\omega/\omega_{des} = 0.6$

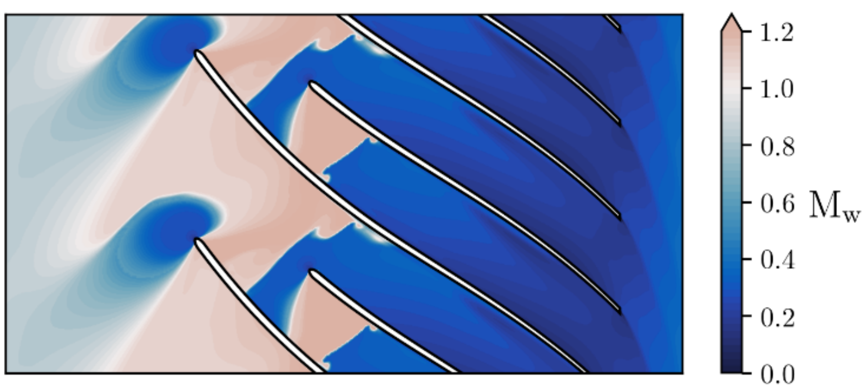

$\phi/\phi_{des} = 1.06$; $\omega/\omega_{des} = 1.0$

Design perspective

- ✓ Cavitation unavoidable in high-load, near-critical sCO_2 compressors operating at $s/s_c < 1$
  - ✓ Blade shape determines rangeability due to cavitation-induced choking
    - ✓ Wrap angle distribution can be optimized to maximize rangeability

Design perspective

- ✓ Cavitation unavoidable in high-load, near-critical sCO_2 compressors operating at $s/s_c < 1$
  - ✓ Blade shape determines rangeability due to cavitation-induced choking
    - ✓ Wrap angle distribution can be optimized to maximize rangeability

→ **Novel compressor blade design tailored on the minimization of cavitation effects**

Design perspective

- ✓ Cavitation unavoidable in high-load, near-critical sCO_2 compressors operating at $s/s_c < 1$
  - ✓ Blade shape determines rangeability due to cavitation-induced choking
    - ✓ Wrap angle distribution can be optimized to maximize rangeability

→ Novel compressor blade design tailored on the minimization of cavitation effects

Design exercise: parametric optimization

- ✓ Blade number reduced to 7 (main) + 7 (splitter) → higher blade load, but wide increase of throat area
- ✓ Reduction of Wrap angle → higher cambering in the front part, but further increase of throat area

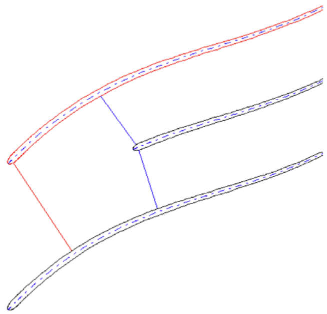

Design perspective

✓ Cavitation unavoidable in high-load, near-critical sCO_2 compressors operating at $s/s_c < 1$

✓ Blade shape determines rangeability due to cavitation-induced choking

✓ Wrap angle distribution can be optimized to maximize rangeability

→ **Novel compressor blade design tailored on the minimization of cavitation effects**

Design exercise: parametric optimization

✓ Blade number reduced to 7 (main) + 7 (splitter) → higher blade load, but wide increase of throat area

✓ Reduction of Wrap angle → higher cambering in the front part, but further increase of throat area

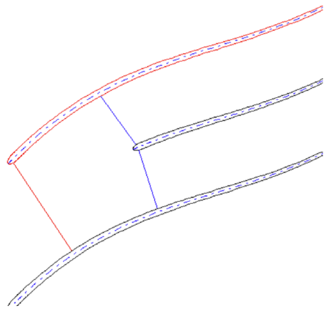

	$\theta = -85^o$	$\theta = -77.5^o$	$\theta = -70^o$	$\theta = -65^o$
η_{TT}	90,46%	90,39%	90,34%	90,18%
η_{TS}	69,23%	69,20%	69,14%	69,02%
β_{TT}	3,41	3,42	3,43	3,44
$mass_{leak}$	16,4%	16,0%	15,5%	15,2%
$C_P vaneless$	0,2726	0,2721	0,2711	0,2707
$P_{stat\,out}$	234,8 bar	235,4 bar	235,7 bar	236,1 bar
Throat (red)	41,165 mm	42,632 mm	44.111 mm	45,092 mm

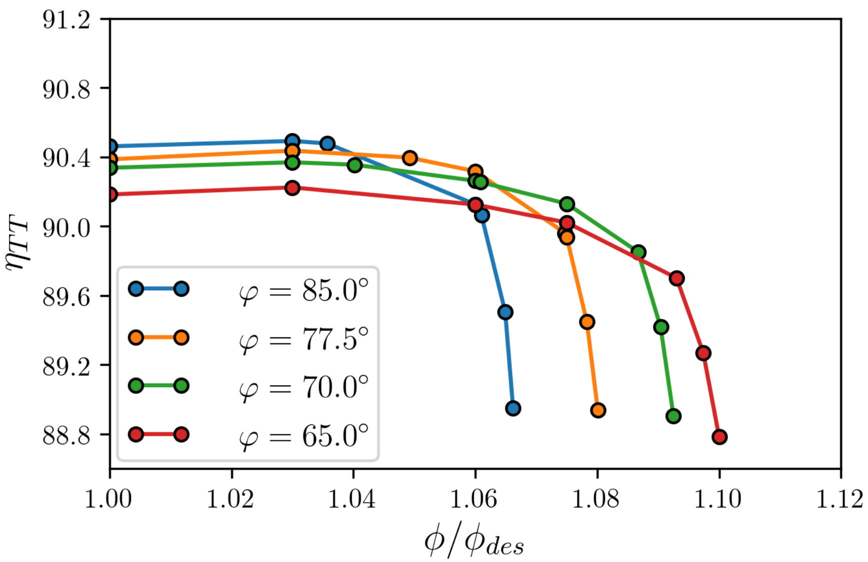

Design perspective

✓ Cavitation unavoidable in high-load, near-critical sCO_2 compressors operating at $s/s_c < 1$

✓ Blade shape determines rangeability due to cavitation-induced choking

✓ Wrap angle distribution can be optimized to maximize rangeability

→ **Novel compressor blade design tailored on the minimization of cavitation effects**

Design exercise: parametric optimization

✓ Blade number reduced to 7 (main) + 7 (splitter) → higher blade load, but wide increase of throat area

✓ Reduction of Wrap angle → higher cambering in the front part, but further increase of throat area

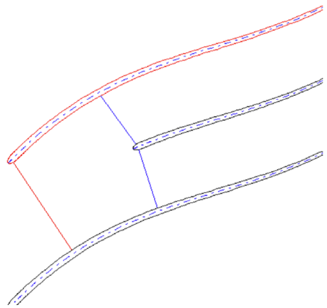

Proper choice of blade shape maximizes throat size increasing by 5% the rangeability, up to $\boldsymbol{\phi/\phi_{des} = 1.1}$

	$\theta = -85^o$	$\theta = -77.5^o$	$\theta = -70^o$	$\theta = -65^o$
η_{TT}	90,46%	90,39%	90,34%	90,18%
η_{TS}	69,23%	69,20%	69,14%	69,02%
β_{TT}	3,41	3,42	3,43	3,44
$mass_{leak}$	16,4%	16,0%	15,5%	15,2%
$C_p vaneless$	0,2726	0,2721	0,2711	0,2707
$P_{stat\,out}$	234,8 bar	235,4 bar	235,7 bar	236,1 bar
Throat (red)	41,165 mm	42,632 mm	44.111 mm	45,092 mm

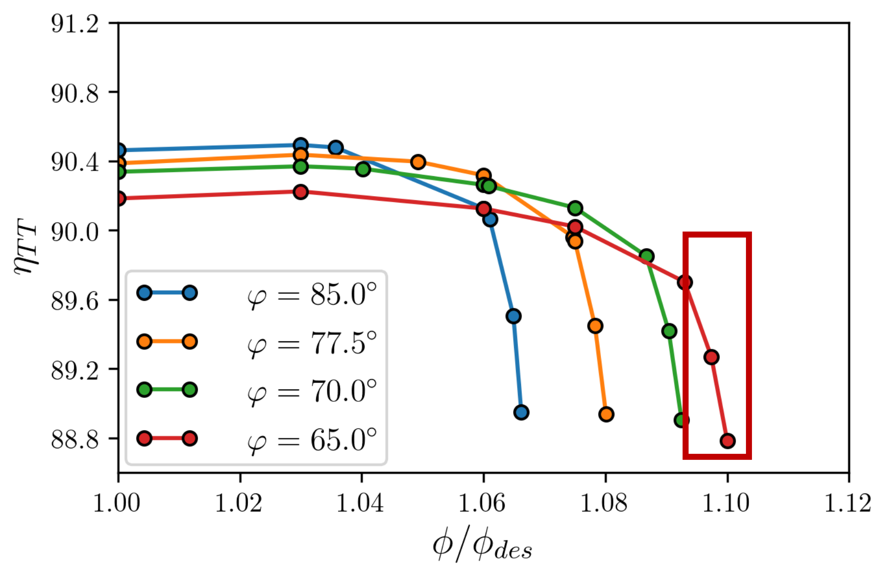

CONCLUSIONS

Design workflow of a high-load sCO_2 compressor

- ✓Cycle optimization, preliminary sizing, aerodynamic blade design

State of the art models for design & analysis sCO_2 compressors

- ✓Mean-line code for preliminary sizing and low-fidelity analysis
- ✓CFD featuring barotropic formulation for two-phase flow simulations

sCO2 compressor aerodynamics in near-critical conditions

- ✓Performance maps between low- and high-fidelity models compared
- ✓Low-fidelity models failure in capturing cavitation-induced choking
- ✓Cavitation-induced choking highly sensitive to angular speed
- ✓Cavitation-induced choking sensitive to blade shape

CONCLUSIONS

Design workflow of a high-load sCO_2 compressor

- ✓Cycle optimization, preliminary sizing, aerodynamic blade design

State of the art models for design & analysis sCO_2 compressors

- ✓Mean-line code for preliminary sizing and low-fidelity analysis
- ✓CFD featuring barotropic formulation for two-phase flow simulations

sCO2 compressor aerodynamics in near-critical conditions

- ✓Performance maps between low- and high-fidelity models compared
- ✓Low-fidelity models failure in capturing cavitation-induced choking
- ✓Cavitation-induced choking highly sensitive to angular speed
- ✓Cavitation-induced choking sensitive to blade shape

→ Novel design strategies can be conceived to enhance the rangeability of near-critical sCO2 compressor

Design and off-design analysis of a highly loaded centrifugal compressor for sCO2 applications operating in near-critical conditions

Alessandro Romei | Paolo Gaetani | Giacomo Persico

giacomo.persico@polimi.it

POLITECNICO MILANO 1863
ENERGY DEPARTMENT

Laboratory of Fluid Machines